Available online at www.sciencedirect.com
ScienceDirect
Mathematics and Computers in Simulation 208 (2023) 535–549
MATHEMATICS AND COMPUTERS IN SIMULATION
www.elsevier.com/locate/matcom

Original articles

Rogue waves and solitons of the generalized modified nonlinear Schrödinger equations

Zehra Pinar Izgi

Department of Mathematics, Tekirdağ Namık Kemal Üniversitesi, Tekirdağ, Turkey

Received 22 November 2022; received in revised form 26 January 2023; accepted 30 January 2023
Available online 3 February 2023

Abstract

Many applications of the classical nonlinear Schrödinger equations with cubic and power nonlinearity are seen in nonlinear optics, plasma physics, superconductivity, propagation of the electric field in optical fibers, self-focusing and collapse of Langmuir waves in plasma physics, to model deep water waves and freak waves in the ocean.
Objectives: In this paper, the generalized form of the modified nonlinear Schrödinger equation is proposed with various nonlinearities.
Methods: Bernoulli equation method, which is one of the ansatz-based methods, is considered to be obtained as the novel soliton solutions of the modified nonlinear Schrödinger equation with various nonlinearities.
Results: With the view of the results, new improvements can happen for applications of the model.

Keywords: Bernoulli equation method; The modified nonlinear Schrödinger equation; Nonlinearities; Solitons

1. Introduction

One of the main nonlinear partial differential equations is the classical nonlinear Schrödinger equation (NSE)

$$i\,\Phi_t + \frac{1}{2}\,\Phi_{xx} + |\Phi|^2\,\Phi = 0, \tag{1}$$

which is seen in the various areas from optics, plasma physics to deep water waves, freak and rogue waves not only on the surface of the ocean but also in fiber optical systems in the literature. New modifications were required due to the inability of classical NSE to model sub picosecond optical dynamics pulses well. Therefore, many modifications have been seen in the literature due to the nonlinearities, two of them are main modifications [8–10,23].

The generalized form of modified nonlinear Schrödinger equation

$$i\,\Phi_t + a\,\Phi_{xx} + F\left(|\Phi|^2\right)\Phi = i\left[\alpha\,\Phi_x + \lambda\left(|\Phi|^{2m}\,\Phi\right)_x + v\left(|\Phi|^{2m}\right)_x\,\Phi\right], \quad i^2 = -1 \tag{2}$$

is given where $\Phi(x,t)$ represents the wave profile in an optical fiber, m, a, α, λ, v are parameters which represent nonlinearity, group velocity dispersion (GVD), inter-modal dispersions (IMD), the self-steepening (SS), nonlinear

E-mail address: zpinar@nku.edu.tr.

https://doi.org/10.1016/j.matcom.2023.01.041

dispersion (ND), respectively. F is a self-phase modulation function which is in a nonlinear form. So, it effects the nonlinearity of Eq. (2).

In this work, we will study on exact solutions of Eq. (2) with respect to the various types of F function that are given by Eq. (3).

$$F(u)=\begin{cases} bu, \text{ Kerr law} \\ bu^n, \text{ Power law} \\ b_1u+b_2u^2, \text{ Parabolic law} \\ b_1u^n+b_2u^{2n}, \text{ Dual-power law} \\ b_1u+b_2u^2+b_3u^3, \text{ Polynomial law} \\ b_1u^n+b_2u^{2n}+b_3u^{3n}, \text{ Triple power law} \\ b_1u+b_2u^2+b_3u^{-2}, \text{ Anti-cubic law} \\ b_1u^n+b_2u^{n+1}+b_3u^{-(n+1)}, \text{ Generalized Anti-cubic law} \\ b_1\sqrt{u}+b_2u, \text{ Quadratic–cubic law} \\ b\,(u)_{xx}, \text{ Non-local law} \\ b_1u+b_2u^2+b_3\,(u)_{xx}, \text{ Parabolic–Nonlocal combo law} \end{cases} \tag{3}$$

Almost all types of modifications are given by Eq. (3). Additionally, the significant point is the generalization of the F function i.e. when all the types given in Eq. (3) wanted to proposed in one function, it may be

$$F(u)=b_1u^n+b_2u^{2n}+b_3u^{3n}+b_4\,(u)_{xx}, \quad n\in R. \tag{4}$$

Since the nonlinear Schrödinger equation (NSE) has the Benjamin–Feir instability [25] proposed as one of the mechanisms for rogue wave generation [6], the NSE has been extensively studied as a model for extreme wave behavior. Many methodologies have been considered to obtain the solutions of various types of nonlinear Schrödinger equation [1–5,7–10,12–14,23,24,31,32,35,36,38,39]. The dark and singular solitons of Schrödinger equation with non-Kerr-law nonlinearity were investigated by Biswas et al. and Jawad et al. [7,35], asymptotic solutions of modified NSE were obtained by Kitaev et al. [9], many works can be seen in Refs. [15,20]. In this work, the novel exact solutions including rogue waves of Eq. (2) for each function F given by Eq. (3) are obtained via Bernoulli approximation method which is ansatz depended method, for details Refs. [26–29] should be read and also, in the second section the brief methodology is given. In third section, the obtained solutions by Bernoulli approximation method are proposed and supported by the 3D-, 2D- and contour plots.

2. Brief of the methodology

As mentioned above, Bernoulli equation method is ansatz-based method like Riccati equation method. Bernoulli equation is best known nonlinear ordinary differential equation (NODE) after Riccati differential equation. The Bernoulli type differential equation is

$$z'(\zeta)=P(\zeta)\,z(\zeta)+Q(\zeta)\,z^2(\zeta), \tag{5}$$

where $P(\zeta)$ and $Q(\zeta)$ are arbitrary functions [33,34] so Eq. (5) is not classical Bernoulli equation. When the arbitrary functions are constant, the equation is reduced to Bernoulli differential equation.

To solve nonlinear partial differential equation (NPDE), firstly NPDE has to be reduced to NODE via wave transformation; secondly using balancing principle the degree of the ansatz $\Phi(\zeta)=\sum_{i=0}^{N}g_iz^i(\zeta)$ i.e. N is determined, where g_i are parameters, it is clear that $z(\zeta)$ is the solution of Bernoulli differential equation. Finally, substitute Bernoulli differential equation and the ansatz into NODE to obtain algebraic system for obtaining the parameters.

As seen in the procedure of the methodology, it is same as the well-known methods like Riccati equation method, tanh method, auxiliary equation method, etc. [11,12,16–19,21,22,30,37,40,41].

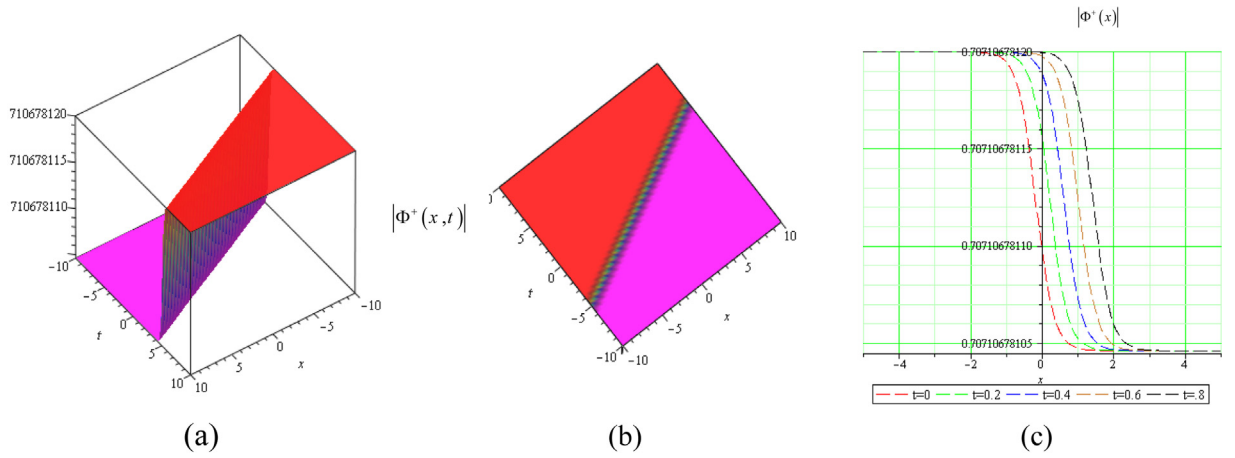

Fig. 1. (a) 3D, (b) contour and (c) 2D plots (at t = 0, 0.2, 0.4, 0.6, 0.8) of the modulus of the exact wave solution of $\Phi^{+}(x,t)$ with Kerr Law when $P=2, \alpha=1, a=1, b=1, \lambda=2, \kappa=-1.5, g_1=2, \theta_0=0, C_1=1$.

3. Solutions

To solve Eq. (2) with the various F function like in Eq. (3), firstly the complex wave transformation $\Phi(x,t) = \Psi(\zeta)\exp(i\varphi(x,t))$ is considered where $\zeta = x-ct$, $\varphi(x,t) = -\kappa x+\omega t+\theta_0$ i.e.

$$\Phi(x,t) = \Psi(x-ct)\exp(i(-\kappa x+\omega t+\theta_0)) \tag{6}$$

and $\kappa, \omega, \theta_0, c$ are frequency, the wave number, phase constant, the velocity of the soliton, respectively.

As a result, Eq. (1) is reduced into two equations due to real and imaginary parts, respectively.

$$a\Psi'' - \left(\omega + a\kappa^2 + \alpha\kappa\right)\Psi + F\left(\Psi^2\right)\Psi - \kappa\lambda\Psi^{2m+1} = 0 \tag{7}$$

where F function is determined in Eq. (4).

$$(c+2a\kappa+\alpha)\Psi' + (\lambda(2m+1)+2mv)\Psi'\Psi^{2m} = 0, \tag{8}$$

which gives two algebraic equations $c+(2a\kappa+\alpha)=0$ and $\lambda(2m+1)+2mv=0$ which will be used in the considered method. The second one is the relation between nonlinearity and self-stepping. Additionally, to satisfy the integrability condition, generally $m=n$ is chosen.

Applying the procedure of Bernoulli equation method as mentioned previous section, the solutions are obtained for each F function, the obtained parameters and 3D-, 2D- and contour plots are given below.

Case 1. Kerr Law when $m=1$.

$$c = -(2a\kappa+\alpha),\ g_0 = \pm P\sqrt{\frac{a}{2(\kappa\lambda-b)}},\quad v = -\frac{3\lambda}{2},\quad \omega = -(a\kappa^2+\alpha\kappa+\frac{1}{2}aP^2),\quad Q = \mp\sqrt{-\frac{b-\kappa\lambda}{2a}}g_1. \tag{9}$$

So, the soliton solution is given by

$$\begin{aligned}\Phi^{\pm}(x,t) &= \pm P\sqrt{\frac{a}{2(\kappa\lambda-b)}} + g_1\left(\frac{P}{PC_1\exp(-P(x+(2a\kappa+\alpha)t)) \mp b_1\sqrt{\frac{\kappa\lambda-b}{2a}}}\right)\\ &\times\exp\left(i\left(-\kappa x-(a\kappa^2+\alpha\kappa+\frac{1}{2}aP^2)t+\theta_0\right)\right).\end{aligned} \tag{10}$$

Fig. 1 represents the exact wave solution as soliton solution given by Eq. (10) with the parameters $P=2, \alpha=1, a=1, b=1, \lambda=2, \kappa=-1.5, g_1=2, \theta_1=0$ when $C_1=1$. The 3D, contour and 2D plots of $\left|\Phi^{+}(x,t)\right|$ are shown in Fig. 1(a), (b) and (c), respectively.

Case 2 Power Law when $m=n=\frac{1}{2}$.

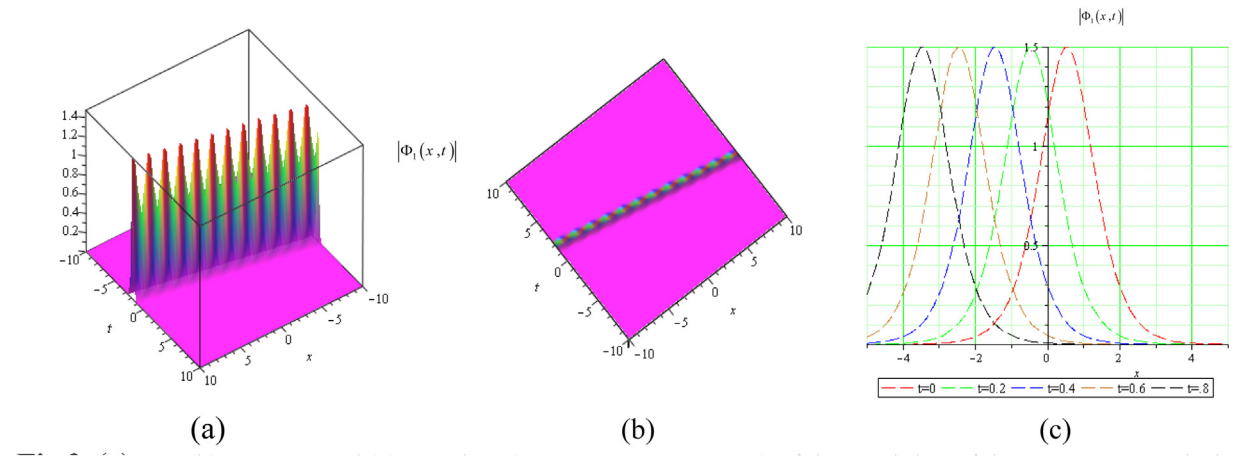

Fig. 2. (a) 3D, (b) contour and (c) 2D plots (at t = 0, 0.2, 0.4, 0.6, 0.8) of the modulus of the exact wave solution as a peaked rogue wave of $\Phi_1(x,t)$ with Power Law when $P=2, \alpha=2, a=1, b=1, \lambda=-2, \kappa=1.5, g_0=1, g_1=2, \theta_0=1, C_1=1$.

The parameters are obtained as;

Set 1.

$$c=-(2a\kappa+\alpha),\ g_0=0,\ g_2=-\frac{b_1^2(b-\kappa\lambda)}{6aP^2},\quad v=-2\lambda,\quad \omega=aP^2-a\kappa^2-\alpha\kappa,\quad Q=-\frac{g_1(b-\kappa\lambda)}{6aP}. \tag{11}$$

Set 2.

$$\begin{aligned} c &= -(2a\kappa+\alpha),\ g_0=-\frac{aP^2}{b-\kappa\lambda},\quad g_2=-\frac{g_1^2(b-\kappa\lambda)}{6aP^2},\quad v=-2\lambda,\quad \omega=aP^2-a\kappa^2-\alpha\kappa,\\ Q &= -\frac{g_1(b-\kappa\lambda)}{6aP}. \end{aligned} \tag{12}$$

When the parameters are substituted, the exact wave solutions are obtained as

$$\Phi_1(x,t)=\left(\frac{b_1P}{PC_1\exp\left(-P(x+(2a\kappa+\alpha)t)\right)-\frac{b_1(b-\kappa\lambda)}{6aP}}\left(\frac{P}{PC_1\exp\left(-P(x+(2a\kappa+\alpha)t)\right)-\frac{b_1(b-\kappa\lambda)}{6aP}}\right)^2\right)\exp\left(i\left(-\kappa x-(aP^2-a\kappa^2-\alpha\kappa)t+\theta_0\right)\right), \tag{13}$$

and

$$\Phi_2(x,t)=\left(-\frac{aP^2}{b-\kappa\lambda}+\frac{b_1P}{PC_1\exp\left(-P(x+(2a\kappa+\alpha)t)\right)-\frac{b_1(b-\kappa\lambda)}{6aP}}\left(\frac{P}{PC_1\exp\left(-P(x+(2a\kappa+\alpha)t)\right)-\frac{b_1(b-\kappa\lambda)}{6aP}}\right)^2\right)\exp\left(i\left(-\kappa x-(aP^2-a\kappa^2-\alpha\kappa)t+\theta_0\right)\right). \tag{14}$$

Fig. 2 represents the exact wave solution given by Eq. (13) with the parameters $P=2, \alpha=2, a=1, b=1, \lambda=-2, \kappa=1.5, g_0=1, g_1=2, \theta_0=1$, when $C_1=1$. The 3D, contour and 2D plots of $|\Phi_1(x,t)|$ are shown in Fig. 2(a), (b) and (c), respectively.

Case 3 Dual-power Law

When $m = 1$, the equation has parabolic law nonlinearity. The parameters are hold as

$$c = -(2a\kappa + \alpha), v = -\frac{3\lambda}{2}, g_0 = \frac{\sqrt{15b_2(-b_1 + \kappa\lambda)}}{5b_2},$$
$$g_1 = \frac{2C_1\sqrt{15b_2(-b_1 + \kappa\lambda)}}{23b_2}\exp\left(-\frac{\zeta(-b_1 + \kappa\lambda)\sqrt{-6b_2a}}{5b_2a}\right)$$

$$Q(\zeta) = \pm\frac{2C_1\sqrt{30b_2(-b_1 + \kappa\lambda)a(b_1 - \kappa\lambda)}}{46b_2a}\exp\left(-\frac{\zeta(-b_1 + \kappa\lambda)\sqrt{-6b_2a}}{5b_2a}\right), \tag{15}$$

$$P(\zeta) = \pm\frac{\sqrt{30b_2(-b_1 + \kappa\lambda)}(3b_1 - 3\kappa\lambda)}{15b_2\sqrt{a(5b_1 - 5\kappa\lambda)}}.$$

As a result, the solution is

$$\Phi(x,t) = \frac{15(\kappa\lambda - b_1)\sqrt{15}\left(\exp\left(\frac{(\kappa\lambda - b_1)(2a\kappa t + \alpha t + x)\sqrt{-6ab_1}}{5ab_2}\right) - \frac{23}{15}\exp\left(\frac{(\kappa\lambda - b_1)(2a\kappa t + \alpha t + x)\sqrt{6b_2(\kappa\lambda - b_1)}}{5b_2\sqrt{-a(\kappa\lambda - b_1)}}\right)\right)}{\sqrt{6b_2(\kappa\lambda - b_1)}\left(125\exp\left(\frac{(\kappa\lambda - b_1)(2a\kappa t + \alpha t + x)\sqrt{-6ab_1}}{5ab_2}\right) - 115\exp\left(\frac{(\kappa\lambda - b_1)(2a\kappa t + \alpha t + x)\sqrt{6b_2(\kappa\lambda - b_1)}}{5b_2\sqrt{-a(\kappa\lambda - b_1)}}\right)\right)}$$
$$\times \exp\left(-i\frac{25b_2(\kappa(x + (a\kappa + \alpha)t) - \theta_0) + 6(\kappa\lambda - b_1)^2 t}{25b_2}\right) \tag{16}$$

Also, if $m = n = \frac{1}{2}$, then the parameters are hold as

$$Q(\zeta) = \pm\frac{g_1\sqrt{-2ab_2}}{2a}, c = -(2a\kappa + \alpha), v = -2\lambda, \omega = -\kappa(a\kappa + \alpha), b_1 = \kappa\lambda, g_0 = 0$$

$$P(\zeta) = \tanh\left(\frac{(\zeta + C_1)\sqrt{a\alpha\kappa - 3ab_2g_0^2 + a\omega + a^2\kappa^2}}{a}\right)\frac{\sqrt{a\alpha\kappa - 3ab_2g_0^2 + a\omega + a^2\kappa^2}}{a}. \tag{17}$$

Hence, the solution is

$$\Phi(x,t) = -\frac{ag_1\exp\left(i\left(-\kappa x - \left(a\kappa^2 + \alpha\kappa\right)t + \theta_0\right)\right)}{-2g_1(x + (2a\kappa + \alpha)t)\sqrt{2a\kappa\lambda} - aC_1}. \tag{18}$$

Fig. 3 represents the rogue waves in periodic form given by Eqs. (16) and (18) with the parameters $a = 1, \alpha = 2, \lambda = 2, \kappa = -1, \theta_0 = 1, g_1 = 1, b_1 = -1, b_2 = 2$ and $a = -1, \alpha = 2, \lambda = 1, \kappa = 1, \theta_0 = 1, g_1 = 1$ when $C_1 = 1, C_2 = 1$, respectively. The 3D, contour and 2D plots of real part of $\Phi(x,t)$ are shown in Fig. 3i–ii (a), (b) and (c) for each solution, respectively.

Case 4 Triple-power law:

When $m = \frac{1}{2}$, the equation has polynomial law nonlinearity. The parameters are hold as

$$P(\zeta) = \mp\frac{(35b_3g_0^4 - 70b_3g_0^5 + b_1)\sqrt{3}}{4\sqrt{-a\left(21b_3g_0^2 - 7b_3g_0^3\right)}}, Q(\zeta) = \pm\frac{g_1^2\sqrt{-3a\left(21b_3g_0^2 - 7b_3g_0^3\right)}}{3a}, c = -(2a\kappa + \alpha), b_2 = -7b_3g_0^3,$$
$$\lambda = -\frac{11291g_0^8b_3^2 - 1106b_1b_3g_0^4 + 3b_1^2}{672\kappa b_3g_0^3}, v = \frac{11291g_0^8b_3^2 - 1106b_1b_3g_0^4 + 3b_1^2}{336\kappa b_3g_0^3},$$
$$\omega = -\frac{7259g_0^8b_3^2 - 434b_1b_3g_0^4 + 3b_1^2 + 672\kappa b_3g_0^2(a\kappa + \alpha)}{672\kappa b_3g_0^3}, \tag{19}$$
$$g_1 = \pm\frac{-105b_3g_0^4 + 3b_1 + \sqrt{\exp\left(\frac{3\xi(-35b_3g_0^4 + b_1)}{4\sqrt{-42ab_3g_0^2}}\right)C_1b_3g_0^4\left(-1152480b_3g_0^4 + 32928b_1\right) + 11025g_0^8b_3^2 - 630b_1b_3g_0^4 + 9b_1^2}}{784b_3g_0^3}$$

Therefore, the solution is

$$\Phi(x,t)=\left(g_0+\left(3\left(-105\,b_3\,g_0^4+3\,b_1+\sqrt{-1152480\,e^{\frac{3\left(-(-2a\kappa-\alpha)t+x\right)\left(-35\,b_3\,g_0^4+b_1\right)}{4\sqrt{-42\,a\,b_3\,g_0^2}}}\_C1\,b_3^2\,g_0^8+11025\,g_0^8\,b_3^2+32928\,e^{\frac{3\left(-(-2a\kappa-\alpha)t+x\right)\left(-35\,b_3\,g_0^4+b_1\right)}{4\sqrt{-42\,a\,b_3\,g_0^2}}}\_C1\,b_1\,b_3\,g_0^4-630\,b_1\,b_3\,g_0^4+9\,b_1^2}\right)\left(-35\,b_3\,g_0^4+b_1\right)\right)\Big/\left(784\,b_3\,g_0^3\left(-105\,e^{\frac{3\left(-(-2a\kappa-\alpha)t+x\right)\left(-35\,b_3\,g_0^4+b_1\right)}{4\sqrt{-42\,a\,b_3\,g_0^2}}}\_C1\,b_3\,g_0^4-\left(-105\,b_3\,g_0^4+3\,b_1+\sqrt{-1152480\,e^{\frac{3\left(-(-2a\kappa-\alpha)t+x\right)\left(-35\,b_3\,g_0^4+b_1\right)}{4\sqrt{-42\,a\,b_3\,g_0^2}}}\_C1\,b_3^2\,g_0^8+11025\,g_0^8\,b_3^2+32928\,e^{\frac{3\left(-(-2a\kappa-\alpha)t+x\right)\left(-35\,b_3\,g_0^4+b_1\right)}{4\sqrt{-42\,a\,b_3\,g_0^2}}}\_C1\,b_1\,b_3\,g_0^4-630\,b_1\,b_3\,g_0^4+9\,b_1^2}\right)^2\Big/10976\,b_3\,g_0^4+3\,e^{\frac{3\left(-(-2a\kappa-\alpha)t+x\right)\left(-35\,b_3\,g_0^4+b_1\right)}{4\sqrt{-42\,a\,b_3\,g_0^2}}}\_C1\,b_1\right)\right)\Big/\left(e^{\left(-\kappa x-\frac{\left(7259\,g_0^8\,b_3^2+672\,a\,\kappa^2\,b_3\,g_0^2-434\,b_1\,b_3\,g_0^4+672\,a\,\kappa\,b_3\,g_0^2+3\,b_1^2\right)t}{672\,b_3\,g_0^2}+\theta_0\right)}\right)^1 \tag{20}$$

Also, if $m=n=\frac{1}{2}$, then the parameters are hold as

$$c=-(2a\kappa+\alpha),\ v=-3\lambda,\ \omega=-\frac{6a\kappa^2g_2+6\alpha\kappa g_2-b_1g_1^2+\kappa\lambda g_1^2}{6g_2},\ b_2=0,\ b_1=0,\ g_0=\frac{g_1^2}{g_2},$$

$$Q(\zeta)=\pm\frac{\sqrt{6ag_2\left(-6b_3g_0^2g_2^2-12b_3g_0g_1^2g_2-b_3g_1^4-3b_2g_0g_2^2-3b_2g_2g_1^2-g_2^2(b_1-\kappa\lambda)\right)}}{6ag_2}. \tag{21}$$

$$P(\zeta)=\pm\frac{g_1\sqrt{6}\left(-5b_1g_2^2+5g_2^2\kappa\lambda-30b_3g_0^2g_2^2+b_3g_1^4-15b_2g_0g_2^2\right)}{30g_2\sqrt{ag_2\left(-6b_3g_0^2g_2^2-12b_3g_0g_1^2g_2-b_3g_1^4-3b_2g_0g_2^2-3b_2g_2g_1^2-g_2^2(b_1-\kappa\lambda)\right)}}$$

With the obtained parameters, the solution is

$$\Phi(x,t)=\frac{g_1^2\exp\left(-i\left(\frac{(6\kappa((a\kappa+\alpha)t+x)-6\theta_0)g_2+g_1^2(\kappa\lambda-b_1)t}{6g_2}\right)\right)\left(g_2\exp\left(\frac{g_1g_2(2a\kappa t+\alpha t+x)\sqrt{6}(\kappa\lambda-b_1)}{6\sqrt{ag_2^3(\kappa\lambda-b_1)}}\right)+C_1g_1\right)^2}{6g_2\left(g_2\exp\left(\frac{g_1g_2(2a\kappa t+\alpha t+x)\sqrt{6}(\kappa\lambda-b_1)}{6\sqrt{ag_2^3(\kappa\lambda-b_1)}}\right)-C_1g_1\right)^2}. \tag{22}$$

Fig. 4 represents the exact wave solutions given by Eqs. (20) and (22) with the parameters $a=0.1,\alpha=-2,\kappa=1,b_1=1,b_3=-0.1,g_0=-1,\theta_0=1,C_1=0.1$ and $a=1,\alpha=2,\lambda=-2,\kappa=1,\theta_0=1,C_1=1,C_2=1,g_1=1,g_2=-1,b_1=1$, respectively. The 3D, contour and 2D plots of real part of $\Phi(x,t)$ are shown in Fig. 4i–ii (a), (b) and (c) for each solution, respectively.

Case 5 Generalized anti-cubic Law:

When $m=\frac{1}{2}$, the equation has anti-cubic law nonlinearity. The parameters are hold as

$$Q(\zeta)=\pm\frac{g_1\sqrt{-2a\left(20g_0^2b_2+b_1\right)}}{2a},\ P(\zeta)=\pm\frac{\left(-3b_1g_0+28b_2g_0^3+\kappa\lambda\right)\sqrt{2}}{3\sqrt{-2a\left(20g_0^2b_2+b_1\right)}},\ g_0=\frac{2\kappa\lambda}{3b_1},$$

$$C_1=\frac{7g_1}{8\exp\left(\pm\frac{2}{3}\zeta\kappa\lambda\sqrt{-\frac{3g_0}{4a\kappa\lambda}}\right)},\ c=-\frac{3a\kappa^2-g_0\kappa\lambda-3\omega}{3\kappa},\ v=-3\lambda,\ \alpha=-\frac{3a\kappa^2+g_0\kappa\lambda+3\omega}{3\kappa} \tag{23}$$

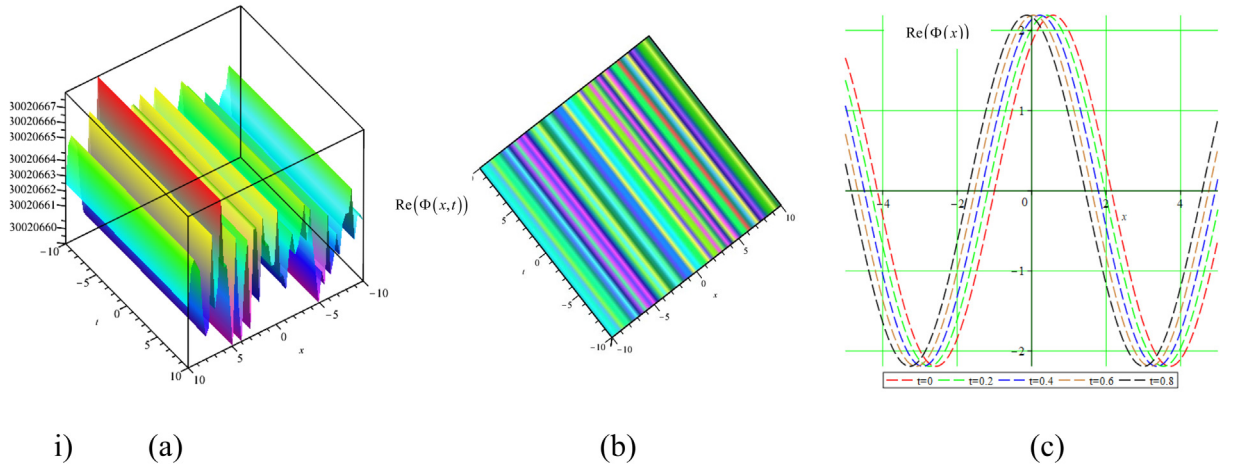

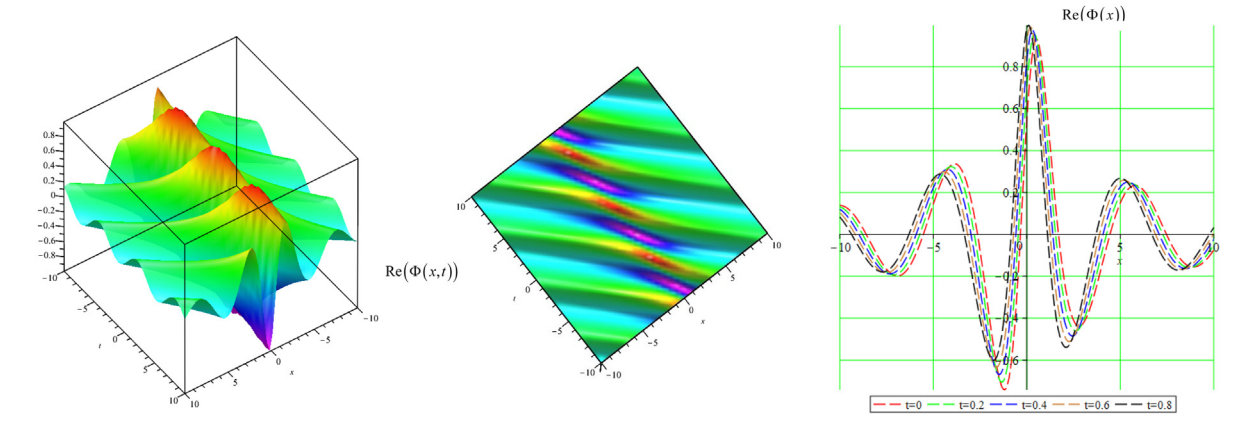

Fig. 3. (i) (a) 3D, (b) contour and (c) 2D plots (at t = 0, 0.2, 0.4, 0.6, 0.8) of the modulus of the exact wave solution of $\Phi(x,t)$ with Parabolic Law when $a=1, \alpha=2, \lambda=2, \kappa=-1, \theta_0=1, g_1=1, b_1=-1, b_2=2$.
(ii) (a) 3D, (b) contour and (c) 2D plots (at t = 0, 0.2, 0.4, 0.6, 0.8) of the modulus of the exact wave solution of $\Phi(x,t)$ with Dual-Power Law when $a=-1, \alpha=2, \lambda=1, \kappa=1, \theta_0=1, g_1=1$ when $C_1=1, C_2=1$, respectively.

So, the solution is

$$\Phi(x,t)=\left(\frac{2\kappa\lambda}{3b_1}+\frac{2g_1\left(\frac{224b_2\kappa^3\lambda^3}{27b_1^3}\kappa\lambda\right)}{\exp\left(-\frac{2\left(\frac{224b_2\kappa^3\lambda^3}{27b_1^3}\kappa\lambda\right)\left(\frac{\left(3a\kappa^2-\frac{2\kappa^2\lambda^2}{3b_1}-3\omega\right)t}{3\kappa}+x\right)}{\sqrt[3]{-2a\left(\frac{112\kappa^2\lambda^2b_2}{9b_1^2}+b_1\right)}}\right)}\right.$$
$$\left.\frac{\left(\frac{196\kappa^2\lambda^2b_2g_1}{9b_1^2}-\frac{21b_1g_1}{8}\right)}{\exp\left(2\kappa\lambda\left(\frac{\left(3a\kappa^2-\frac{2\kappa^2\lambda^2}{3b_1}-3\omega\right)t}{3\kappa}+x\right)\sqrt{\frac{-1}{2ab_1}}/3\right)}+\frac{112\kappa^2\lambda^2b_2g_1}{3b_1^2}+3b_1g_1\right)$$
$$\times\exp\left(i\left(-\kappa x+\omega t+\theta_0\right)\right) \tag{24}$$

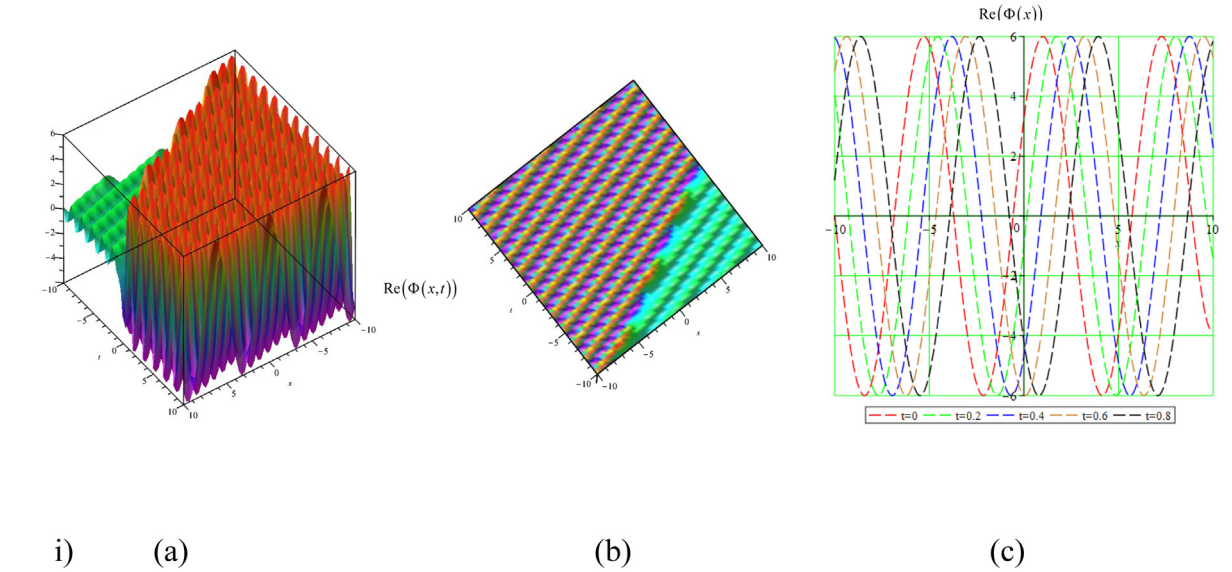

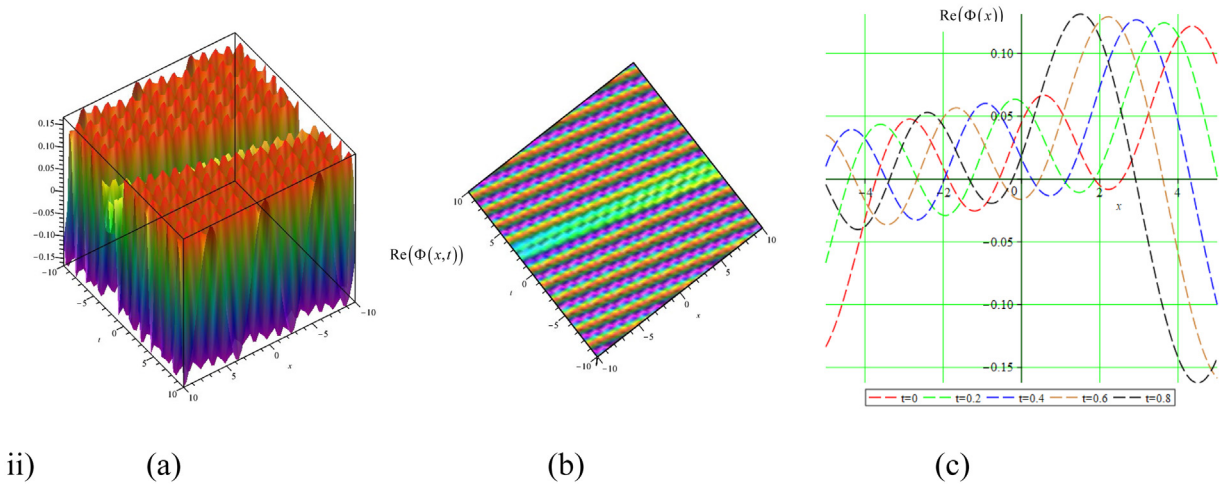

Fig. 4. (i) (a) 3D, (b) contour and (c) 2D plots (at t = 0, 0.2, 0.4, 0.6, 0.8) of the modulus of the exact wave solution of $\Phi(x,t)$ with Polynomial Law when $b_1 = 1, b_3 = 1, g_0 = -1, \theta_0 = 1$.
(ii) (a) 3D, (b) contour and (c) 2D plots (at t = 0, 0.2, 0.4, 0.6, 0.8) of the modulus of the exact wave solution in a rogue wave form of $\Phi(x,t)$ with Triple-Power Law when $a = 1, \alpha = 2, \lambda = -2, \kappa = 1, \theta_0 = 1, C_1 = 1, C_2 = 1, g_1 = 1, g_2 = -1, b_1 = 1$, respectively.

Also, if $m = n = \frac{1}{2}$, then the parameters are hold as

$$P(\zeta) = \zeta^2, Q(\zeta) = \frac{4\zeta g_1 b_2}{3\left(-5\zeta b_2^5 b_b\right)^{1/6}}, C_1 = -\frac{g_1 b_2\left(16\pi 3^{5/6}\zeta^2 - 24\Gamma\left(\frac{2}{3}\right)\Gamma\left(\frac{1}{3}, -\frac{2}{5}\right)3^{1/3}\zeta^2 + 45\Gamma\left(\frac{2}{3}\right)e^{2/5}\right)}{54\left(-5\zeta b_2^5 b_b\right)^{1/6}\Gamma\left(\frac{2}{3}\right)},$$

$$c = -(2a\kappa + \alpha), v = -2\lambda, b_1 = a\kappa^2 + \frac{32}{45}\zeta a + \alpha\kappa + \kappa\lambda + \omega, g_0 = \frac{\left(-5\zeta b_2^5 b_b\right)^{1/6}}{b_2} \quad (25)$$

As a result, the solution is obtained as

$$\Phi(x,t) = \frac{\left(-5\left(x-(2a\kappa+\alpha)t\right)b_2^5 b_b\right)^{1/6}\exp\left(i\left(\kappa x+\omega t+\theta_0\right)\right)}{b_2} + \left(9g_1\Gamma\left(\frac{2}{3}\right)\left(-\left(x-(2a\kappa+\alpha)t\right)^3\right)^{1/3}\exp\left(\frac{\left(x-(2a\kappa+\alpha)t\right)^3}{3}\right)\right)\exp\left(i\left(\kappa x+\omega t+\theta_0\right)\right) \times \left(\frac{\begin{pmatrix}-24\left(x-(2a\kappa+\alpha)t\right)^3 g_1 5^{5/6} b_2\Gamma\left(\frac{1}{3},-\frac{(x-(2a\kappa+\alpha)t)^3}{3}\right)3^{1/3}\Gamma\left(\frac{2}{3}\right)+16\left(x-(2a\kappa+\alpha)t\right)^3 g_1 5^{5/6} b_2 3^{5/6}\pi \\ +g_1\left(-\left(x-(2a\kappa+\alpha)t\right)^3\right)^{1/3}5^{5/6}b_2\left(\left(x-(2a\kappa+\alpha)t\right)^2\left(16\pi 3^{5/6}-24\Gamma\left(\frac{2}{3}\right)\Gamma\left(\frac{1}{3},-\frac{2}{5}\right)3^{1/3}\right)+45\Gamma\left(\frac{2}{3}\right)e^{2/5}\right)\end{pmatrix}}{30\left(-\left(x-(2a\kappa+\alpha)t\right)b_3 b_2^5\right)^{1/6}}\right)^{-1} \tag{26}$$

Fig. 5 represents the exact wave solutions given by Eqs. (24) and (26) with the parameters $a=1,\alpha=-2,\omega=-1,\lambda=-2,\kappa=1,\theta_0=1,b_1=1,b_2=1,g_1=1$ and $a=-1,\alpha=-0.5,b_2=1,b_3=1,\omega=1,\kappa=-1,\theta_0=1,g_1=1$, respectively. The 3D, contour and 2D plots of real part of $\Phi(x,t)$ are shown in Fig. 5i–ii (a), (b) and (c) for each solution, respectively.

Case 6 Quadratic–cubic Law: The parameters are obtained as

$$P(\zeta)=-1, a=\frac{2}{3}bg_0^2, c=-\frac{4}{3}bg_0^2\kappa-\alpha, v=\frac{b}{\kappa}, \omega=\frac{2}{3}bg_0^2(1-\kappa)-\alpha\kappa, \lambda=-\frac{2b}{3\kappa}, \quad C_1=-\frac{g_1\left(-i\sqrt{2}+2\right)}{6g_0\exp(\zeta)}, Q(\zeta)=\pm\frac{g_1\sqrt{2a\kappa\lambda}}{2a} \tag{27}$$

and the solution is hold as

$$\Phi(x,t)=\frac{g_0^2C_1\exp\left(-\frac{i\left(\left(a_2g_0^2+(a\kappa+\alpha)\kappa\right)t+\kappa x-\theta_0\right)\sqrt{-ab_2}-((2a\kappa+\alpha)t+x)g_0b_2\sqrt{2}}{2\sqrt{-ab_2}}\right)}{g_0C_1\exp\left(\frac{((2a\kappa+\alpha)t+x)g_0b_2\sqrt{2}}{2\sqrt{-ab_2}}\right)-g_1}. \tag{28}$$

Fig. 6 represents the exact wave solutions given by Eq. (28) with the parameters $\alpha=0.2,b=-1,g_0=-0.1,g_1=-1,\kappa=1,\theta_0=2$. The 3D, contour and 2D plots of real part of $\Phi(x,t)$ are shown in Fig. 6(a), (b) and (c) for each solution, respectively.

Case 7 Parabolic–Nonlocal combo Law: In the view of the previous cases, two types of nonlinearities are obtained. In the case of $m=1$ and $b_1=b_2=0$, the equation has nonlocal law nonlinearity. The parameters are hold as

$$P(\zeta)=-\frac{bg_1+2bg_0Q(\zeta)\pm\sqrt{b^2g_1^2-4b^2g_0g_1Q(\zeta)+4b^2g_0^2Q(\zeta)^2+2b\kappa\lambda g_1^2-4baQ(\zeta)^2}}{2bg_1}, \quad Q(\zeta)=\frac{7g_1\left(65-7\sqrt{145}\right)}{576g_0}, v=\frac{b\left(2933+413\sqrt{145}\right)}{5184\kappa}, \quad \omega=\frac{47}{54}bg_0^2-\frac{59}{27}bg_0^2\frac{\left(65-7\sqrt{145}\right)}{288}+\frac{40}{21}bg_0^2\kappa^2-\alpha\kappa, \quad \lambda=-\frac{b\left(2933+413\sqrt{145}\right)}{7776\kappa}, g_1=-\frac{15g_0C_1\left(169+15\sqrt{145}\right)}{508\exp\left(-\frac{7\zeta}{-1+\sqrt{145}}\right)}. \tag{29}$$

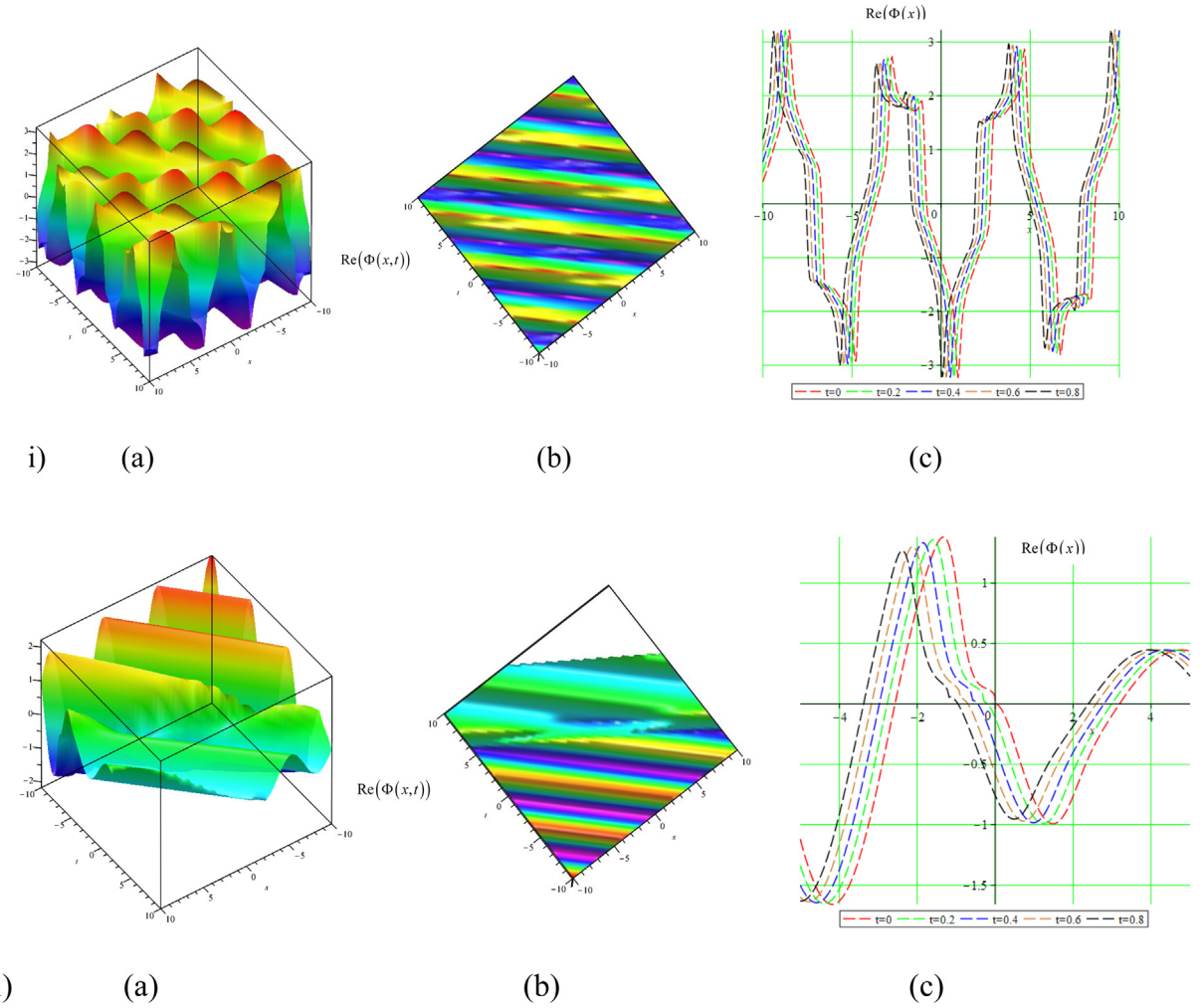

Fig. 5. (i) (a) 3D, (b) contour and (c) 2D plots (at t = 0, 0.2, 0.4, 0.6, 0.8) of the modulus of the exact wave solution in a periodic form of $\Phi(x,t)$ with Anti-cubic Law when $a=1, \alpha=-2, \omega=-1, \lambda=-2, \kappa=1, \theta_0=1, b_1=1, b_2=1, g_1=1$.
(ii) (a) 3D, (b) contour and (c) 2D plots (at t = 0, 0.2, 0.4, 0.6, 0.8) of the modulus of the exact wave solution in one-fold rogue wave form of $\Phi(x,t)$ with generalized anti-cubic Law when $a=-1, \alpha=-0.5, b_2=1, b_3=1, \omega=1, \kappa=-1, \theta_0=1, g_1=1$, respectively.

and the solution is hold as

$$\Phi(x,t) = \left(g_0 + g_1 \frac{S\left(4Abg_0g_1 - \kappa\lambda g_1^2 + 2A^2a\right)}{\left(2A^2bg_0g_1 + Abg_1^2 + Ag_1\sqrt{4A^2b^2g_0^2 - 4Ab^2g_0g_1 + 2b\kappa\lambda g_1^2 - 4A^2ab + b^2g_1^2}\right)S + C_1\left(4Abg_0g_1 - \kappa\lambda g_1^2 + 2A^2a\right)} \right)$$
$$\times \exp\left(i\left(\kappa x + \omega t + \theta_0\right)\right),$$
$$S = \exp\left(-\frac{\left(2Abg_0 + bg_1 - \sqrt{4A^2b^2g_0^2 - 4Ab^2g_0g_1 + 2b\kappa\lambda g_1^2 - 4A^2ab + b^2g_1^2}\right)(x - ct)}{2bg_1} \right).$$

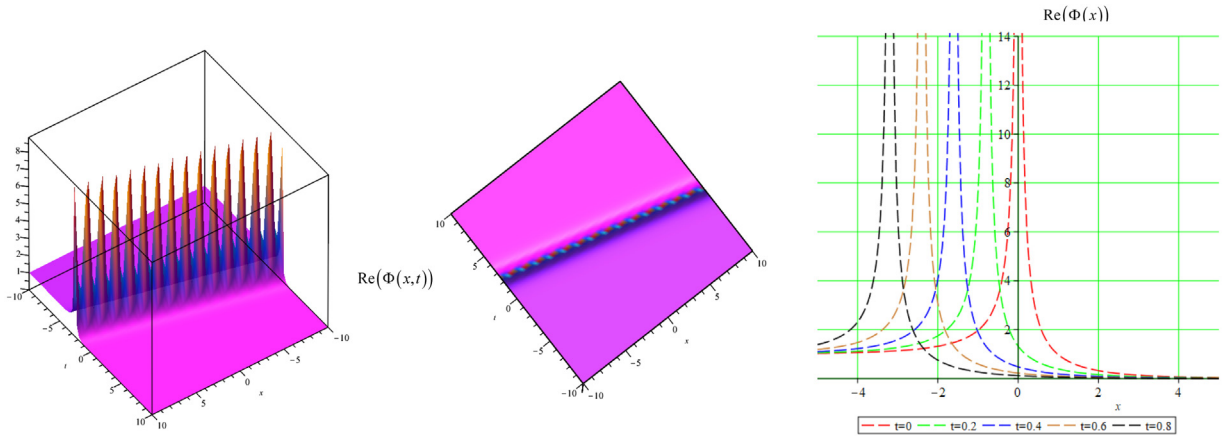

Fig. 6. (a) 3D, (b) contour and (c) 2D plots (at t = 0, 0.2, 0.4, 0.6, 0.8) of the modulus of the exact wave solution of $\Phi(x,t)$ as a peaked rogue wave form with Quadratic–cubic Law when $\alpha = 0.2, b = -1, g_0 = -0.1, g_1 = -1, \kappa = 1, \theta_0 = 2$.

(30)

Also, if $m = 1$ and $b_1 \neq 0, b_2 \neq 0, b_3 \neq 0$, the equation has parabolic–nonlocal law nonlinearity. The parameters are hold as

$$\begin{aligned} &Q(\zeta) = \pm\frac{g_1\sqrt{-b_2b_3}}{2b_3},\ P(\zeta) = \mp\frac{b_2g_0}{\sqrt{-b_2b_3}},\ c = -(2a\kappa+\alpha),\ v = -\frac{3\lambda}{2},\ \omega = -a\kappa^2 - \alpha\kappa - b_2g_0^4 \\ &g_0 = -\frac{\left(a\kappa^2+\alpha\kappa+\omega\right)b_3\sqrt{-2\left(2b_3\sqrt{-b_3b_2}-ab_2\right)}}{2b_3\sqrt{-b_3b_2}-ab_2}, \\ &\omega = \frac{\left(-4b_3^3 - 4b_3^2\left(a\kappa^2+\alpha\kappa\right) + 2ab_3\left(\kappa\lambda - b_1\right) + a^2b_2\right)\sqrt{-b_3b_2} + 4b_3^2\left(\left(\kappa\lambda - b_1\right) + ab_2\right)}{4b_3^2\sqrt{-b_3b_2}}. \end{aligned} \tag{31}$$

Therefore, the solution is given as

$$\begin{aligned} \Phi(x,t) = &\left(-\frac{\left(a\kappa^2+\alpha\kappa+\omega\right)b_3\sqrt{-2\left(2b_3\sqrt{-b_3b_2}-ab_2\right)}}{2b_3\sqrt{-b_3b_2}-ab_2} - \frac{g_1\sqrt{\left(a\kappa^2+\alpha\kappa+\omega\right)b_3\sqrt{-2\left(2b_3\sqrt{-b_3b_2}-ab_2\right)}}}{\left(2b_3\sqrt{-b_3b_2}-ab_2\right)\exp\left(-\frac{2b_2b_3\left(a\kappa^2+\alpha\kappa+\omega\right)\left((2\kappa a+\alpha)t+x\right)C_1}{\left(2b_3\sqrt{-b_3b_2}-ab_2\right)\sqrt{-b_3b_2}} - g_1\right)}\right) \\ &\times \exp\left(i\left(-\kappa x + \omega t + \theta_0\right)\right) \end{aligned} \tag{32}$$

Fig. 7 represents the exact wave solutions given by Eqs. (30) and (32) with the parameters $\alpha = 0.2, b = 2, \kappa = 1, \theta_0 = 1, g_0 = -0.5, C_1 = 1$ and $a = 1, \alpha = -2, \lambda = -2, \kappa = 1, \theta_0 = 1, b_1 = -1, b_2 = 1, b_3 = 1, g_1 = -1, C_1 = -1$, respectively. The 3D, contour and 2D plots of real part of $\Phi(x,t)$ are shown in Fig. 7i–ii (a), (b) and (c) for each solution, respectively.

Case 8 Generalized form for $F(u) = b_1u^n + b_2u^{2n} + b_3u^{3n} + b_4(u)_{xx}$ includes previous nonlinearity cases which are given following Table 1.

Now, Eq. (3) is considered for the nonzero coefficients b_1, b_2, b_3, b_4, n and the given procedure is applied to obtain the solutions of Eq. (1) with Eq. (3).

Applying the given procedure, the solution set is obtained as follows;

$$c = -(2a\kappa+\alpha),\ v = -\frac{3\lambda}{2},\ \omega = -\kappa\left(a\kappa+\alpha\right),\ b_1 = \frac{3\kappa\lambda b_4 + ab_2}{3b_4}. \tag{33}$$

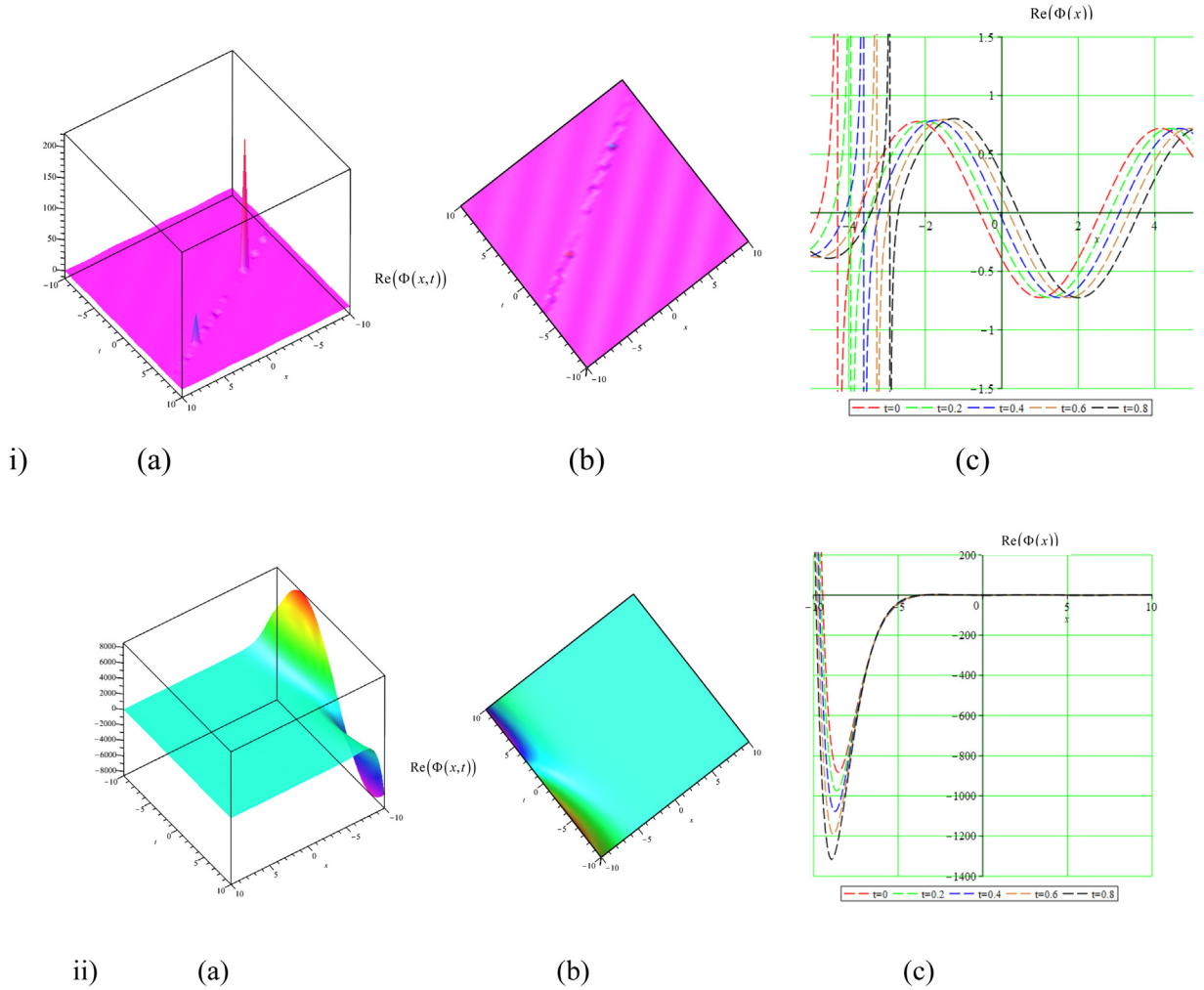

Fig. 7. (i) (a) 3D, (b) contour and (c) 2D plots (at t = 0, 0.2, 0.4, 0.6, 0.8) of the modulus of the exact wave solution of $\Phi(x,t)$ with nonlocal Law when $\alpha = 0.2, b = 2, \kappa = 1, \theta_0 = 1, g_0 = -0.5, C_1 = 1$.
(ii) (a) 3D, (b) contour and (c) 2D plots (at t = 0, 0.2, 0.4, 0.6, 0.8) of the modulus of the exact wave solution of $\Phi(x,t)$ with parabolic-nonlocal-combo Law when $a = 1, \alpha = -2, \lambda = -2, \kappa = 1, \theta_0 = 1, b_1 = -1, b_2 = 1, b_3 = 1, g_1 = -1, C_1 = -1$, respectively.

The solution is hold

$$\Phi(x,t) = \left(g_0 + \frac{2g_1 g_0 b_2}{2g_0 b_2 C_1 \exp\left(\frac{2g_0 b_2((2\kappa a+\alpha)t+x)}{\sqrt{-6b_4\left(21b_3 g_0^2+b_2\right)}}\right) - 21b_3 g_0^2 g_1 - b_2 g_1} \right) \exp\left(i\left(-\kappa\left(x+(a\kappa+\alpha)t\right)+\theta_0\right)\right). \tag{34}$$

Fig. 8 represents the exact wave solutions as rogue wave given by Eq. (34) with the parameters $a = 1, \alpha = -2, \lambda = -2, \kappa = 5, b_2 = 1, b_3 = -1, b_4 = -1, g_0 = 0.00001, g_1 = -2, C_1 = -2, \theta_0 = -2$. The 3D, contour and 2D plots of real part of $\Phi(x,t)$ are shown in Fig. 8(a), (b) and (c) for each solution, respectively.

Table 1
Reductions of Eq. (3) due to coefficients b_1, b_2, b_3, b_4, n.

$b_2 = b_3 = b_4 = 0, b_1 = b$	bu^n, Power law
$b_3 = b_4 = 0, n = 1$	$b_1 u + b_2 u^2$, Parabolic law
$b_3 = b_4 = 0$	$b_1 u^n + b_2 u^{2n}$, Dual-power law
$b_4 = 0, n = 1$	$b_1 u + b_2 u^2 + b_3 u^3$, Polynomial law
$b_4 = 0$	$b_1 u^n + b_2 u^{2n} + b_3 u^{3n}$, Triple power law
$b_3 = b_4 = 0, n = \frac{1}{2}$	$b_1 \sqrt{u} + b_2 u$, Quadratic–cubic law
$b_1 = b_2 = b_3 = 0, b_4 = b$	$b\,(u)_{xx}$, Non-local law
$b_3 = 0, n = 1$	$b_1 u + b_2 u^2 + b_4\,(u)_{xx}$, Parabolic–Nonlocal combo law

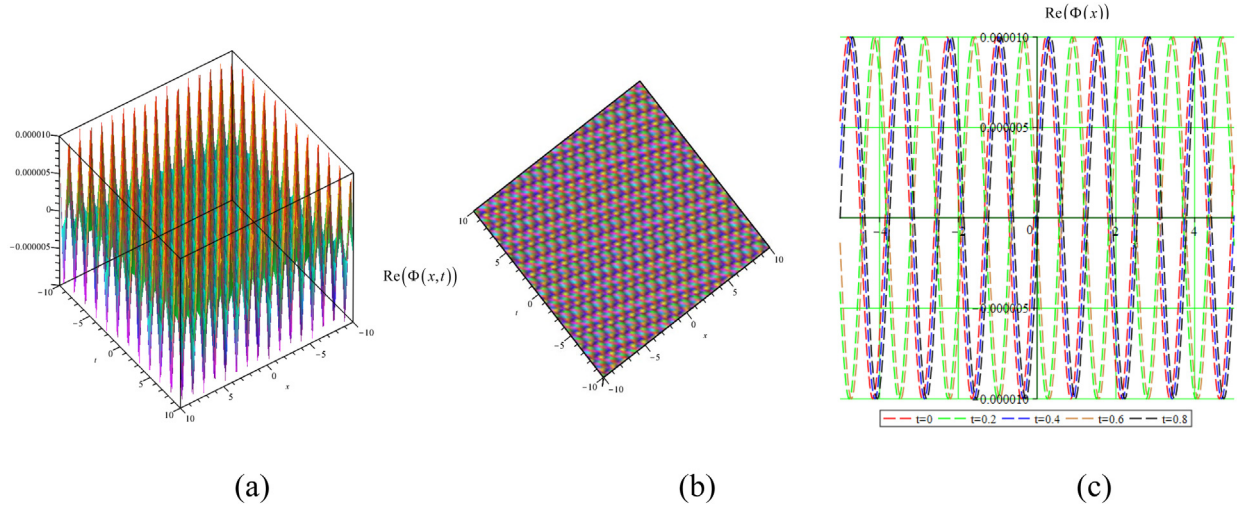

Fig. 8. (a) 3D, (b) contour and (c) 2D plots (at t = 0, 0.2, 0.4, 0.6, 0.8) of the modulus of the exact wave solution of $\Phi(x,t)$ as a periodic rogue wave form with $F(u) = b_1 u^n + b_2 u^{2n} + b_3 u^{3n} + b_4\,(u)_{xx}$ when $a = 1, \alpha = -2, \lambda = -2, \kappa = 5, b_2 = 1, b_3 = -1, b_4 = -1, g_0 = 0.00001, g_1 = -2, C_1 = -2, \theta_0 = -2$.

The solution sets include one of the reduced cases when $b_3 = 0$ that correspond to parabolic non-local combo law. Additionally, one new case is obtained for $b_1 = 0, b_3 = 0$

$$C_1 = \frac{5g_1}{14g_0 \exp\left(\frac{g_0\zeta\sqrt{6}}{3b_4\sqrt{-(b_2b_4)^{-1}}}\right)}, a = -\frac{b_4\left(-4b_2g_0^2 + 3\kappa\lambda\right)}{b_2}, c = -\frac{8\kappa b_2 b_4 g_0^2 - 6\kappa^2\lambda b_4 + \alpha b_2}{b_2},$$

$$v = -\frac{3\lambda}{2}, \omega = -\frac{4\kappa^2 b_2 b_4 g_0^2 - b_2^2 g_0^4 - 3\kappa^3\lambda b_4 + \kappa\lambda b_2 g_0^2 + \alpha\kappa b_2}{b_2}, b_1 = 0, b_3 = 0. \tag{35}$$

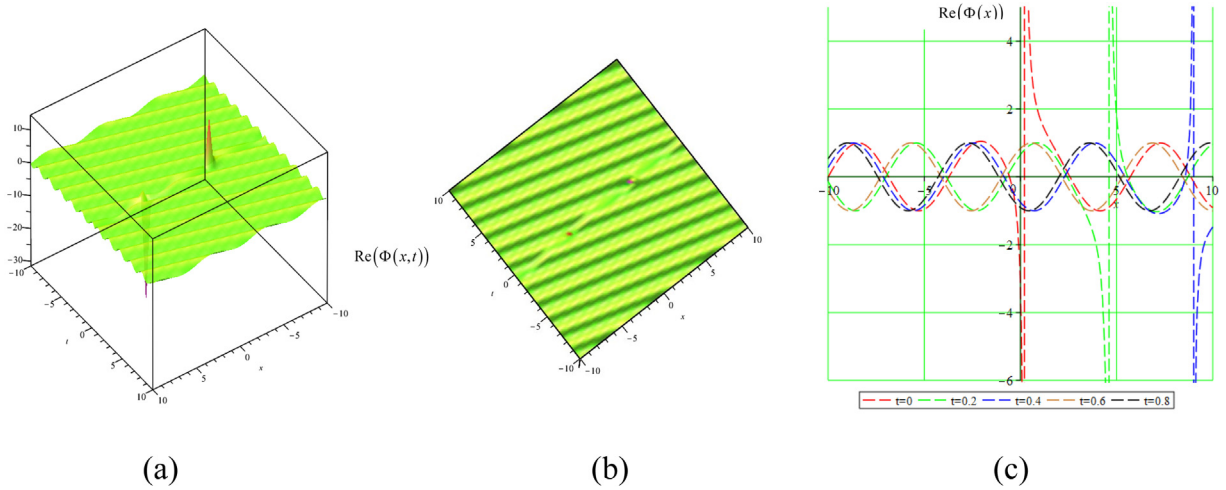

Fig. 9. (a) 3D, (b) contour and (c) 2D plots (at t = 0, 0.2, 0.4, 0.6, 0.8) of the modulus of the exact wave solution of $\Phi(x,t)$ as one-fold rogue wave form with $F(u) = b_2 u^{2n} + b_4 (u)_{xx}$ when $\alpha = -2, \lambda = -2, \kappa = 1, \theta_0 = 1, b_2 = 1, b_4 = -1, g_0 = 1, g_1 = -1$.

and its solution is given as follows

$$\Phi(x,t) = \left(\frac{g_0 \left(5\exp\left(-\frac{2g_0\sqrt{6}\left(-\left(\left(\frac{4\kappa b_4 g_0^2}{3} + \frac{\alpha}{6} \right) t + \frac{x}{6} \right) b_2 + \kappa^2 \lambda b_4 t \right)}{\sqrt{-b_2 b_4}} \right) + 7\exp\left(\frac{g_0\sqrt{6}\left(8\kappa t b_2 b_4 g_0^2 - 6\kappa^2 \lambda t b_4 + \alpha t b_2 + x b_2 \right)}{3\sqrt{-b_2 b_4}} \right) \right)}{5\exp\left(-\frac{2g_0\sqrt{6}\left(-\left(\left(\frac{4\kappa b_4 g_0^2}{3} + \frac{\alpha}{6} \right) t + \frac{x}{6} \right) b_2 + \kappa^2 \lambda b_4 t \right)}{\sqrt{-b_2 b_4}} \right) - 7\exp\left(\frac{g_0\sqrt{6}\left(8\kappa t b_2 b_4 g_0^2 - 6\kappa^2 \lambda t b_4 + \alpha t b_2 + x b_2 \right)}{3\sqrt{-b_2 b_4}} \right)} \right) \times \exp\left(i \frac{\left(g_0^4 b_2^2 + \left(\left(4\kappa^2 b_4 g_0^2 + \alpha \right) \kappa t - \kappa x + \theta_0 \right) b_2 \right) + 3\kappa^3 t \lambda b_4}{b_2} \right). \tag{36}$$

Fig. 9 represents the exact wave solutions as one-fold rogue waves given by Eq. (36) with the parameters $\alpha = -2, \lambda = -2, \kappa = 1, \theta_0 = 1, b_2 = 1, b_4 = -1, g_0 = 1, g_1 = -1$. The 3D, contour and 2D plots of real part of $\Phi(x,t)$ are shown in Fig. 9. (a), (b) and (c) for each solution, respectively.

4. Conclusion

The generalized form of modified nonlinear Schrödinger equation (Eq. (2)) has been modified due to the inadequacy of the classical NSE. Therefore, many modifications of NSE have been seen in the literature due to the nonlinearities. In this paper, the generalized form of modified nonlinear Schrödinger equation with various types of nonlinearities is proposed. As a significant point, generalized nonlinearity is proposed which includes many nonlinearities. To obtain exact solutions, Bernoulli equation method, which is one of the ansatz-based methods, is considered. The rogue waves, solitons, and periodic solutions are all represented as a result. The results will be considered for the new application areas of the generalized form of modified NSE.

References

[1] R. Abazari, Application of extended tanh function method on KdV-Burgers equation with forcing term, Romanian J. Phys. 59 (1–2) (2014) 3–11.
[2] R. Abazari, S. Jamshidzadeh, Exact solitary wave solutions of the complex Klein–Gordon equation, Optik- Int. J. Light Electron Opt. 126 (19) (2015) 1970–1975.
[3] R. Abazari, S. Jamshidzadeh, A. Biswas, Solitary wave solutions of coupled Boussinesq equation, Complexity 15 (S2) (2016) 151–155.
[4] N.N. Akhmediev, A. Ankiewicz, Solitons: Nonlinear Pulses and Beams, Vol. 4, Chapman & Hall, London, 1997.
[5] L. Akinyemi, M. Mirzazadeh, S.A. Badri, K. Hosseini, Dynamical solitons for the perturbated Biswas–Milovic equation with Kudryashov's law of refractive index using the first integral method, J. Modern Opt. 69 (3) (2022) 172–182.
[6] T.B. Benjamin, J. Feir, The disintegration of wave trains on deep water Part 1, Theory. J. Fluid Mech. 27 (1967) 417–430.

[7] A. Biswas, A.J.M. Jawad, Q. Zhou, Resonant optical solitons with anti-cubic nonlinearity, Optik 157 (2018) 525–531.
[8] J.R. de Oliveira, M.A. de Moura, Analytical solution for the modified nonlinear Schrödinger equation describing optical shock formation, Phys. Rev. E 57 (4) (1998) 4751–4756.
[9] J.C. DiFranco, P.D. Miller, The semiclassical modified nonlinear Schrödinger equation I: Modulation theory and spectral analysis, Physica D 237 (2008) 947–997.
[10] E.V. Doktorov, The modified nonlinear Schrödinger equation: facts and artefacts, Eur. Phys. J. B 29 (2002) 227–231.
[11] W. Gao, H. Rezazadeh, Z. Pinar, H.M. Baskonus, S. Sarwar, G. Yel, Novel explicit solutions for the nonlinear Zoomeron equation by using newly extended direct algebraic technique, Opt. Quantum Electron. 52 (1) (2020) 1–13.
[12] B. Ghanbari, K.S. Nisar, M. Aldhaifallah, Abundant solitary wave solutions to an extended nonlinear Schrödinger's equation with conformable derivative using an efficient integration method, Adv. Difference Equ. 2020 (1) (2020) 1–25.
[13] B. Ghanbari, A. Yusuf, D. Baleanu, The new exact solitary wave solutions and stability analysis for the (2+ 1)-dimensional Zakharov–Kuznetsov equation, Adv. Difference Equ. 2019 (1) (2019) 1–15.
[14] K. Hosseini, E. Hincal, M. Mirzazadeh, S. Salahshour, O.A. Obi, F. Rabiei, A nonlinear Schrödinger equation including the parabolic law and its dark solitons, Optik 273 (2023) 170363.
[15] K. Hosseini, E. Hincal, S. Salahshour, M. Mirzazadeh, K. Dehingia, B.J. Nath, On the dynamics of soliton waves in a generalized nonlinear Schrödinger equation, Optik 272 (2023) 170215.
[16] K. Hosseini, M. Mirzazadeh, J.F. Gómez-Aguilar, Soliton solutions of the Sasa–Satsuma equation in the monomode optical fibers including the beta-derivatives, Optik 224 (2020) 165425.
[17] K. Hosseini, M. Mirzazadeh, M. Ilie, S. Radmehr, Dynamics of optical solitons in the perturbed Gerdjikov–Ivanov equation, Optik 206 (2020) 164350.
[18] K. Hosseini, M. Mirzazadeh, J. Vahidi, R. Asghari, Optical wave structures to the Fokas–Lenells equation, Optik 207 (2020) 164450.
[19] A. Houwe, S. Abbagari, Y. Salathiel, M. Inc, S.Y. Doka, K.T. Crépin, D. Baleanu, Complex traveling-wave and solitons solutions to the Klein–Gordon–Zakharov equations, Results Phys. (2020) 103127.
[20] O.A. Ilhan, J. Manafian, M. Shahriari, Lump wave solutions and the interaction phenomenon for a variable-coefficient Kadomtsev–Petviashvili equation, Comput. Math. Appl. 78 (8) (2019) 2429–2448.
[21] M. Inc, A.I. Aliyu, A. Yusuf, D. Baleanu, New solitary wave solutions and conservation laws to the Kudryashov–Sinelshchikov equation, Optik 142 (2017) 665–673.
[22] S. Jamshidzadeh, R. Abazari, Solitary wave solutions of three special types of Boussinesq equations, Nonlinear Dynam. 88 (4) (2017) 2797–2805.
[23] A.J.M. Jawad, M.J. Abu-AlShaeer, F.B. Majid, A. Biswas, Q. Zhou, M. Belic, Optical soliton on perturbation with exotic non-Kerr law nonlinearities, Optik 158 (2018) 1370–1379.
[24] C. Kharif, E. Pelinovsky, Physical mechanisms of the rogue wave phenomenon, Eur. J. Mech. B/Fluids 22 (6) (2003) 603–634.
[25] A.V. Kitaev, A.H. Vartanian, Asymptotics of solutions to the modified nonlinear Schrödinger equation: Solitons on a nonvanishing continuous background, SIAM J. Math. Anal. 30 (4) (1999) 787–832.
[26] J.G. Liu, M. Eslami, H. Rezazadeh, M. Mirzazadeh, The dynamical behavior of mixed type lump solutions on the (3+1)-dimensional generalized Kadomtsev–Petviashvili–Boussinesq equation, Int. J. Nonlinear Sci. Numer. Simul. (2020) http://dx.doi.org/10.1515/ijnsns-2018-0373.
[27] J. Manafian, Novel solitary wave solutions for the (3+ 1)-dimensional extended Jimbo–Miwa equations, Comput. Math. Appl. 76 (5) (2018) 1246–1260.
[28] J. Manafian, S. Heidari, Periodic and singular kink solutions of the Hamiltonian amplitude equation, Adv. Math. Models Appl 4 (2) (2019) 134–149.
[29] J. Manafian, O.A. Ilhan, A.A. Alizadeh, Periodic wave solutions and stability analysis for the KP-BBM equation with abundant novel interaction solutions, Phys. Scr. 95 (6) (2020) 065203.
[30] K. Munusamy, C. Ravichandran, K.S. Nisar, B. Ghanbari, Existence of solutions for some functional integrodifferential equations with nonlocal conditions, Math. Methods Appl. Sci. 43 (17) (2020) 10319–10331, 30.
[31] S. Nestor, A. Houwe, G. Betchewe, S.Y. Doka, A series of abundant new optical solitons to the conformable space–time fractional perturbed nonlinear Schrödinger equation, Phys. Scr. 95 (8) (2020) 085108.
[32] C. Park, M.M. Khater, A.H. Abdel-Aty, R.A. Attia, H. Rezazadeh, A.M. Zidan, A.B. Mohamed, Dynamical analysis of the nonlinear complex fractional emerging telecommunication model with higher-order dispersive cubic-quintic, Alex. Eng. J. 59 (3) (2020) 1425–1433.
[33] Z. Pinar, Analytical studies for the Boiti–Leon–Monna–Pempinelli equations with variable and constant coefficients, Asymptot. Anal. (2019) 1–9, (Preprint).
[34] Z. Pinar, Analytical results of morphochemical electrodeposition model, Iran. J. Sci. Technol. Trans. A Sci. 44 (4) (2020) 1131–1136.
[35] Z. Pinar, Similarities and exact solutions of transonic gas flow model, Modern Phys. Lett. B (2020) 2050363.
[36] Z. Pinar, H. Rezazadeh, M. Eslami, Generalized logistic equation method for Kerr law and dual power law Schrödinger equations, Opt. Quantum Electron. 52 (12) (2020) 1–16.
[37] G. Rahman, K.S. Nisar, B. Ghanbari, T. Abdeljawad, On generalized fractional integral inequalities for the monotone weighted Chebyshev functionals, Adv. Difference Equ. 2020 (1) (2020) 1–19.
[38] H. Rezazadeh, R. Abazari, M.M.A. Khater, M. Inc, D. Baleanu, New optical solitons of conformable resonant nonlinear Schrödinger's equation, Front. Phys. 8 (332) (2020).
[39] N. Savaissou, B. Gambo, H. Rezazadeh, A. Bekir, S.Y. Doka, Exact optical solitons to the perturbed nonlinear Schrödinger equation with dual-power law of nonlinearity, Opt. Quantum Electron. 52 (318) (2020).
[40] H.M. Srivastava, D. Baleanu, J.A.T. Machado, M.S. Osman, H. Rezazadeh, S. Arshed, H. Günerhan, Traveling wave solutions to nonlinear directional couplers by modified Kudryashov method, Phys. Scr. 95 (7) (2020).
[41] F. Tchier, A.I. Aliyu, A. Yusuf, Dynamics of solitons to the ill-posed Boussinesq equation, Eur. Phys. J. Plus 132 (3) (2017) 136.